

Core RNA Polymerase from *E. coli* Induces a Major Change in the Domain Arrangement of the σ^{70} Subunit

Sandhya Callaci, Ewa Heyduk, and Tomasz Heyduk*
Edward A. Doisy Department of Biochemistry and
Molecular Biology
St. Louis University Medical School
St. Louis, Missouri 63104

Summary

Luminescence resonance energy transfer measurements were used to show that binding of *E. coli* core RNA polymerase induced major changes in interdomain distances in the σ^{70} subunit. The simplest model describing core-induced changes in σ^{70} involves a movement of the conserved region 1 by ~ 20 Å and the conserved region 4.2 by ~ 15 Å with respect to conserved region 2. The core-induced movement of region 1 (autoinhibition domain) and region 4.2 (DNA-binding domain) provides structural rationale for allosteric regulation of σ^{70} DNA binding properties by the core and suggests that this regulation may not only involve directly the autoinhibition domain of σ^{70} but also could involve a modulation of spacing between DNA-binding domains of σ^{70} induced by binding of core RNAP.

Introduction

RNA polymerase from *Escherichia coli* is a multisubunit enzyme composed of two α subunits, large β and β' subunits, and the σ subunit. In the cell, two major forms of the polymerase are found: core enzyme (subunit composition $\alpha_2\beta\beta'$) and holoenzyme (subunit composition $\alpha_2\beta\beta'\sigma$) (Burgess et al., 1969; Burgess and Travers, 1970; Record et al., 1996). The core polymerase is capable of transcription elongation but is unable to initiate transcription at specific promoter sites. The initiation of transcription at specific promoter sites is carried out by the holoenzyme (Burgess et al., 1969; Hinkle and Chamberlin, 1972; Record et al., 1996). Therefore, σ subunit is responsible for the promoter recognition by *E. coli* RNA polymerase. However, free σ^{70} is not able to bind specifically at promoter DNA sites (Wellman and Meares, 1991). This was shown by studies with polypeptide fragments σ^{70} to be due to the autoinhibition of σ^{70} DNA binding activity by the N-terminal domain of σ^{70} (Dombroski et al., 1992, 1993a). A model of regulation of σ^{70} DNA binding activity by the core enzyme was proposed based on these data. In this model, the N-terminal domain of σ^{70} was proposed to be located in the free protein such that it would sterically block the access of promoter DNA to DNA-binding domains of σ^{70} (regions 2.4 and 4.2). Binding of σ^{70} to the core enzyme was proposed to induce a movement of the N-terminal domain to "unmask" σ^{70} DNA-binding domains allowing the protein to recognize promoter DNA (Dombroski et al., 1993b). In this model,

the core enzyme acts as an allosteric modulator of σ^{70} DNA binding activity. This model suggests that binding of σ^{70} to the core should produce a large scale movement of σ^{70} domains.

Conformational changes of σ^{70} induced by interaction with the core enzyme were first observed by Wu et al. (1976). More recently, we have shown that conformation of conserved domains of σ^{70} that were suggested to participate in core-induced structural change (regions 1, 2.4, and 4.2) was indeed affected by the core enzyme (Callaci et al., 1998). Also, the core enzyme induced conformational changes in σ^{70} that could be detected in the region of the protein responsible for binding the nontemplate single-stranded DNA (Callaci and Heyduk, 1998).

In this work, we investigated the nature of core-induced conformational changes in σ^{70} and addressed directly the question of whether the core enzyme does indeed induce a large scale movement of σ^{70} domains as predicted by the model (Dombroski et al., 1993b). The approach taken was to introduce luminescence donors and acceptors to different conserved domains of the protein and to use luminescence resonance energy transfer measurements (LRET) (Selvin and Hearst, 1994; Selvin et al., 1994; Selvin, 1996) to monitor distances between these domains in free σ^{70} and in σ^{70} -core enzyme complex. We observed a major rearrangement of σ^{70} domains consistent with the proposed model. In addition, it was discovered that as a result of core polymerase binding, DNA-binding domains of σ^{70} moved away from each other such that their spatial separation in the holoenzyme became much more compatible with ~ 17 bp separation of -10 and -35 elements of promoter DNA. We propose that this movement of DNA-binding domains of σ^{70} could be an important mechanism by which the ability of σ^{70} to recognize promoter DNA is regulated.

Results

Donor-Acceptor-Labeled Double-Cysteine Mutants of σ^{70}

The overall design of our experiments was to incorporate luminescence donors and fluorescence acceptors into specific locations in the σ^{70} and to use the resonance energy transfer between donor and acceptor to measure interdomain distances in free σ^{70} and σ^{70} bound to the core enzyme. Incorporation of a donor into one specific domain of the protein and the acceptor into some other domain of the same protein is a difficult problem. We used Eu^{3+} chelate, $(\text{Eu}^{3+})\text{DTPA-AMCA-maleimide}$ (Heyduk and Heyduk, 1997, 1998), as a donor since the unique luminescence properties of europium chelates greatly facilitate observation and determination of energy transfer in systems where stoichiometric labeling with donor and acceptor is not possible (Selvin and Hearst, 1994; Selvin et al., 1994; Selvin, 1996; Heyduk and Heyduk, 1997). We engineered, using site-directed mutagenesis, pairs of unique reactive cysteine residues

* To whom correspondence should be addressed (e-mail: heydukt@wpogate.slu.edu).

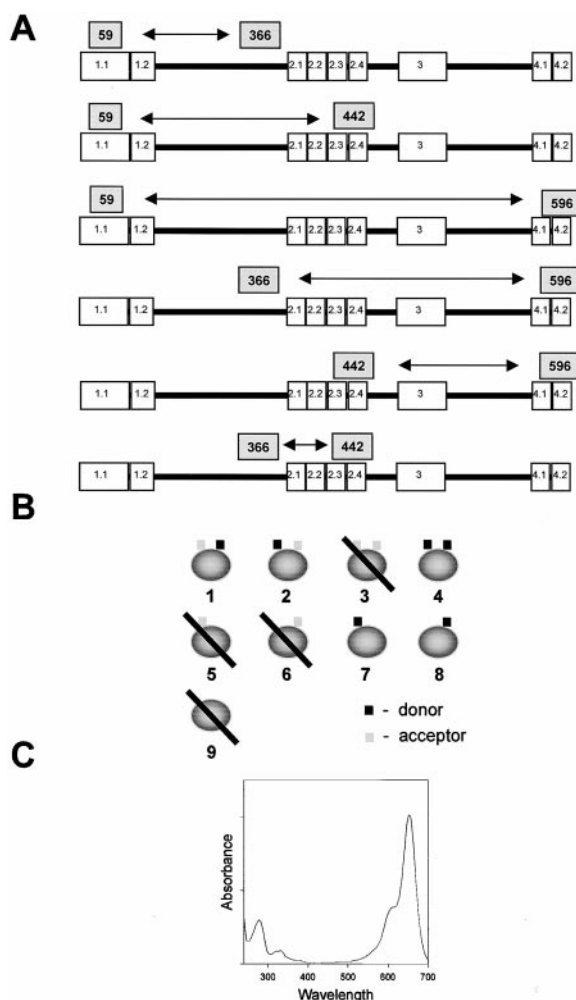


Figure 1. Design for LRET Experiments

(A) Localization of reactive cysteine residues in double-cysteine mutants of σ^{70} . Positions of cysteine residues are indicated by shaded boxes. Conserved regions of σ^{70} are shown as white boxes with numbers identifying each region as defined by Lonetto et al. (1992).

(B) Schematic representation of all possible products of the donor-acceptor modification scheme employed in this report. The products whose contribution to emission in microseconds after excitation pulse is eliminated by time gating are crossed out.

(C) An example of absorption spectrum of donor ((Eu^{3+})DTPA-AMCA-maleimide) and acceptor (Cy5-maleimide) labeled σ^{70} . The spectrum shown is for [S366C, S442C] σ^{70} mutant.

into domains of σ^{70} chosen as desired targets of modification with donors and acceptors (Figure 1A). These double-cysteine mutants of σ^{70} were modified with thiol-reactive donor ((Eu^{3+})DTPA-AMCA-maleimide) and thiol-reactive acceptor (Cy5 maleimide; Callaci et al., 1998) in a random manner, thus producing a mixture of all possible products of such modification (Figure 1B). Only products 1 and 2 (Figure 1B) contain donor and acceptor in a configuration suitable for energy transfer. However, due to a microsecond lifetime of europium chelate donor and nanosecond lifetime of the acceptor, a signal from several species illustrated in Figure 1B could be easily eliminated. A signal from species 3, 5,

and 6 is eliminated by time gating, that is, nanosecond fluorescence of directly excited acceptors decays to zero shortly after the excitation pulse and does not contribute to emission-measured microseconds after the excitation pulse (Selvin and Hearst, 1994; Selvin et al., 1994; Selvin, 1996; Heyduk and Heyduk, 1997). Also, emission of directly excited acceptors in products 1 and 2 is eliminated in the same way. Thus, the decay observed at 617 nm (donor decay) should be a sum of a decay of unquenched donor (no LRET, products 4, 7, and 8) and a decay of the donor engaged in LRET (products 1 and 2). In addition, any emission of the acceptor observed in a microsecond time range could be only due to excitation of the acceptor through energy transfer from the donor and should decay with the lifetime(s) of a donor engaged in energy transfer with the acceptor (Selvin and Hearst, 1994; Selvin et al., 1994; Selvin, 1996; Heyduk and Heyduk, 1997). Thus, fitting simultaneously decays of donor and sensitized acceptor, decay components due to energy transfer can be determined even if their amplitudes are small and their lifetimes are close to lifetimes of unquenched donors (Heyduk and Heyduk, 1998). Figure 1C shows an example of a typical absorbance spectrum of donor and acceptor-labeled σ^{70} . The absorbance peaks characteristic for protein (~ 280 nm), for (Eu^{3+})AMCA-DTPA donor (~ 328 nm), and Cy5 acceptor (~ 647 nm) can be identified showing that the random labeling scheme used to prepare donor-acceptor-labeled protein was successful.

Luminescence Decays of Labeled σ^{70}

Luminescence decays of σ^{70} labeled only with (Eu^{3+})DTPA-AMCA-maleimide (donor-only samples) were rigorously single exponential (Figure 2A). Also, with donor-only σ^{70} , no emission at 670 nm (wavelength of sensitized acceptor emission) was observed (Figure 2C). In contrast, the decay of the donor in donor-acceptor-labeled σ^{70} was not single exponential, and the presence of fast-decaying component(s) was apparent (Figure 2B). The appearance of the fast-decaying component(s) in the donor decay was accompanied by the appearance of a large fast-decaying sensitized acceptor signal (Figure 2C). Thus, the fast decaying component(s) was due to energy transfer between donor and acceptor in donor-acceptor-labeled σ^{70} . In principle, the observed energy transfer could also be intermolecular in nature, particularly if some aggregation of labeled σ^{70} could occur. However, all luminescence decay experiments were performed with proteins that were purified on a sizing column, making the presence of a significant amount of the aggregates unlikely. In addition, in a control experiment in which various ratios of σ^{70} labeled with donor-only and σ^{70} labeled with acceptor-only were mixed, no energy transfer was observed (data not shown). Thus, under conditions used for LRET experiments, the observed energy transfer was between donor and acceptor located on the same σ^{70} molecule.

Decay data for donor-acceptor-labeled σ^{70} were analyzed as described previously (Heyduk and Heyduk, 1998). Donor and sensitized acceptor decays were fitted simultaneously to a three-exponential decay equation. The slowest decay time (τ_3) was the same as the lifetime

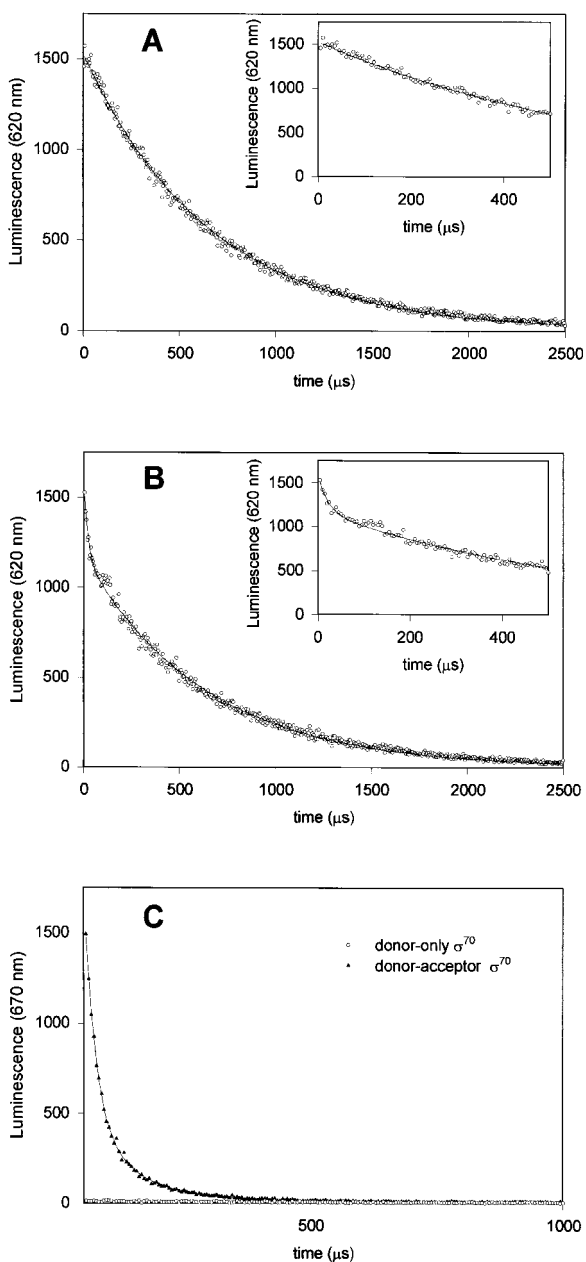


Figure 2. Luminescence Decays of Donor-Only and Donor-Acceptor σ^{70}

Luminescence decay curves for donor-only σ^{70} (A and C) in comparison to donor-acceptor σ^{70} (B and C). The data shown are for [S366C, S442C] σ^{70} mutant. (A) donor decay of donor-only σ^{70} ; (B) donor decay in donor-acceptor σ^{70} . Insets in (A) and (B) show the first 500 μ s of decay curves. Solid lines show nonlinear regression of the data to a single exponential decay equation (A) and triple-exponential decay equation (B), as described in the text. (C) Sensitized acceptor decay curves for donor-only σ^{70} (circles) and donor-acceptor σ^{70} (triangles).

of a donor-only sample, and thus, we attributed this decay component to products of σ^{70} modification that contained donor but no acceptor (products 4, 7, and 8 in Figure 1B). Two lifetimes (τ_1 and τ_2) were necessary to adequately describe the fast-decaying portion of the decay curve. For all LRET calculations presented here,

Table 1. Summary of LRET Results for Free σ^{70}

σ^{70} Protein	τ_d (μ s) ^a	τ_{da} (μ s) ^b	E	R (\AA) ^c
[A59C, S366C] σ^{70}	611 \pm 4	39 \pm 17	0.94 \pm 0.03	35 \pm 3
[A59C, S442C] σ^{70}	653 \pm 7	33 \pm 9	0.95 \pm 0.02	34 \pm 2
[A59C, R596C] σ^{70}	623 \pm 5	34 \pm 6	0.95 \pm 0.02	34 \pm 1
[S366C, S442C] σ^{70}	660 \pm 3	44 \pm 11	0.93 \pm 0.02	35 \pm 2
[S366C, R596C] σ^{70}	632 \pm 4	70 \pm 16	0.89 \pm 0.03	39 \pm 3
[S442C, R596C] σ^{70}	659 \pm 4	45 \pm 7	0.93 \pm 0.02	36 \pm 2

^a Lifetimes of donor-only σ^{70} samples.

^b The average of τ_1 and τ_2 (see Results) for donor-acceptor labeled σ^{70} samples.

^c The errors shown were calculated taking into account only the error of lifetime determination. The actual errors of distance determination are very likely to be higher due, for example, to possible uncertainty of orientation factor value. The actual errors are difficult to estimate quantitatively but are likely to be \sim 12% (the maximal error due to uncertainty of the orientation factor).

we used the weighted average of two fast-decaying components (τ_1 and τ_2) as discussed previously (Heyduk and Heyduk, 1998).

The luminescence lifetimes for all double-cysteine mutants of σ^{70} modified with donor-only and with donor and acceptor were used to calculate interdomain distances (Table 1). The only parameter used in these calculations that cannot be determined experimentally is the orientation factor (κ^2) (Selvin, 1995). We have assumed 2/3 for κ^2 , which is characteristic for completely randomized orientation of donor and acceptors. A possible error of distance measurements due to this assumption is small (\leq 12%) in the case of europium chelates used as donors because of their long lifetimes and the depolarization of emission caused by multiple electronic transitions (Selvin and Hearst, 1994; Selvin et al., 1994; Selvin, 1996; Heyduk and Heyduk, 1997).

Luminescence Decays of Labeled σ^{70} Bound to the Core RNAP

The luminescence decays of donor-only σ^{70} remained single exponential in σ^{70} bound to the core RNAP (data not shown). The effect of core-binding on luminescence decays of donor-acceptor-labeled σ^{70} is illustrated in Figure 3. The fast-decaying portion of the curve in free σ^{70} (Figure 3A) was not observed in the decay of σ^{70} bound to the core RNAP (Figure 3B). The analysis of the decay curve by nonlinear fitting to a three-exponential decay curve revealed that the apparent disappearance of the fast-decaying portion of the curve was due to a major increase in the lifetimes of fast-decaying components (τ_1 and τ_2). The simplest interpretation of the core RNAP effect on luminescence lifetimes of labeled σ^{70} shown in Figure 3 is that the distance between the donor and acceptor in this σ^{70} was increased upon σ^{70} binding to the core RNAP, resulting in a decrease in energy transfer and an increase in τ_1 and τ_2 . Similar effects of core binding were observed with other σ^{70} proteins although the extent of lifetimes changes was different for different proteins (Table 2). The measured lifetimes were used to calculate distances between domains of σ^{70} in complex with the core RNAP (Table 2). Comparison to corresponding distances in the free protein (Table 1) shows that a major increase in distances (10–21 \AA) was

Table 2. Summary of LRET Results for Core-Bound σ^{70}

σ^{70} Protein	τ_d (μ S) ^a	τ_{da} (μ S) ^b	E	R (\AA) ^c
[A59C, S366C] σ^{70}	624 \pm 1	292 \pm 26	0.52 \pm 0.05	54 \pm 2
[A59C, S442C] σ^{70}	653 \pm 1	163 \pm 23	0.75 \pm 0.04	46 \pm 2
[A59C, R596C] σ^{70}	650 \pm 7	306 \pm 26	0.51 \pm 0.05	55 \pm 2
[S366C, S442C] σ^{70}	633 \pm 2	81 \pm 7	0.88 \pm 0.02	39 \pm 1
[S366C, R596C] σ^{70}	602 \pm 3	243 \pm 27	0.62 \pm 0.05	51 \pm 2
[S442C, R596C] σ^{70}	634 \pm 4	238 \pm 5	0.64 \pm 0.02	50 \pm 1

^a Lifetimes of donor-only σ^{70} samples.

^b The average of τ_1 and τ_2 (see Results) for donor-acceptor-labeled σ^{70} samples.

^c The errors shown were calculated taking into account only the error of lifetime determination. The actual errors of distance determination are very likely to be higher due, for example, to possible uncertainty of orientation factor value. The actual errors are difficult to estimate quantitatively but are likely to be \sim 12% (the maximal error due to uncertainty of the orientation factor).

observed for all but one σ^{70} protein. Only the distance between residue 366 and 442 was not changed significantly (within limits of experimental error) upon binding of σ^{70} to the core enzyme.

Luminescence probes used as donors in this work are unusual compared to the standard fluorescence probes.

Their luminescence lifetimes are extremely long (microseconds) (Heyduk and Heyduk, 1997). The local and segmental motions in proteins occur with nanosecond correlation times. Within the microsecond time scale of europium chelate emission, there is ample time for the protein to experience all the local and segmental motions. Thus, the distance measured by energy transfer using europium chelate as a donor most likely reflects the distance of the closest approach of donor and acceptor rather than the average distance between them. Therefore, for one selected σ^{70} protein ([S442C, R596C] σ^{70}), we have also determined whether the change in energy transfer upon σ^{70} binding to core RNAP could be also recorded using a fluorescence donor-acceptor pair with nanosecond lifetimes of the excited state. The energy transfer with such probes is sensitive to changes in average distance between a donor and an acceptor. The σ^{70} protein was labeled with a mixture of donor (CPM) and acceptor (DABMI) in molar ratio 1:3. The purified labeled protein contained both the donor and the acceptor as shown by the presence of absorbance peaks at \sim 390 nm (CPM) and \sim 460 nm (DABMI) in a spectrum of the labeled protein (Figure 4A). Fluorescence emission measurements with labeled free and core-bound σ^{70} revealed a significant increase of donor

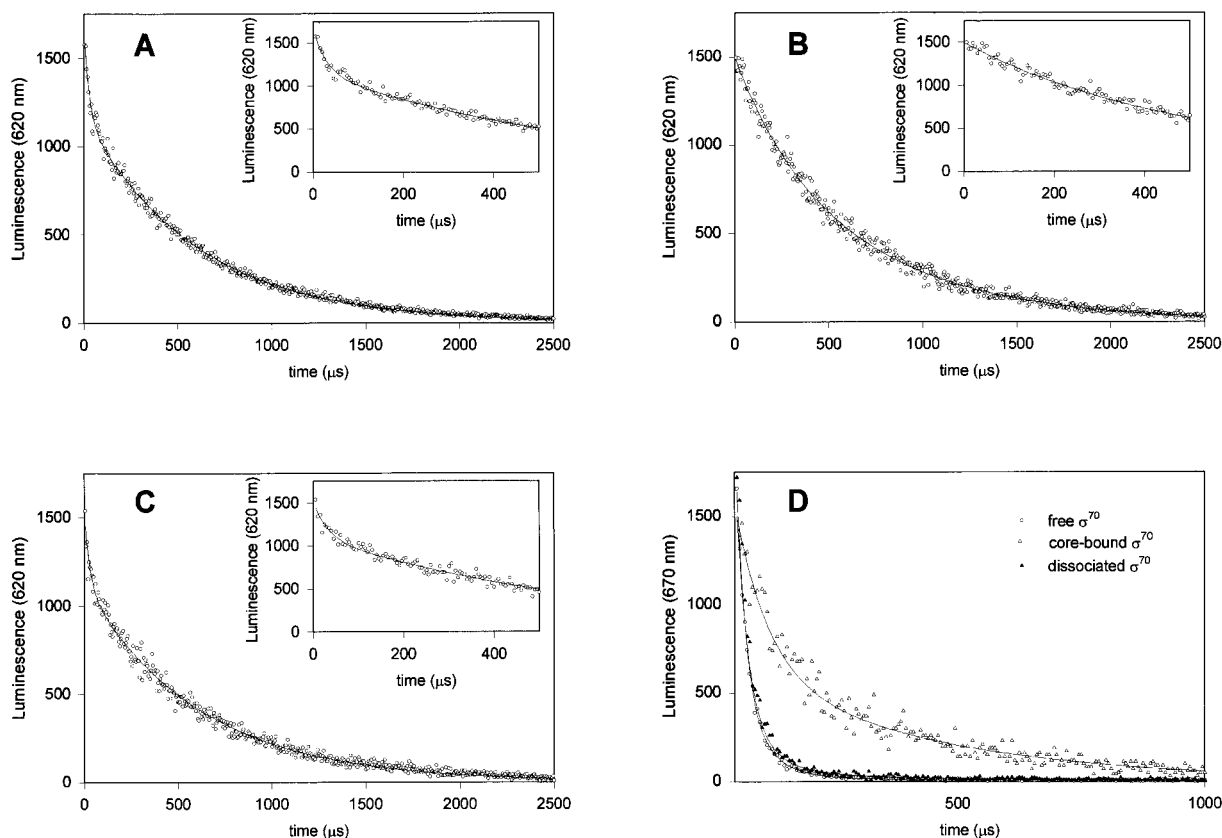


Figure 3. The Effect of Core RNAP on Luminescence Decay of Donor-Acceptor σ^{70}

(A) Free donor-acceptor σ^{70} . (B) Donor-acceptor σ^{70} in complex with the core RNAP. (C) Donor-acceptor σ^{70} dissociated from the holoenzyme (as described in Experimental Procedures) with the excess of unlabeled σ^{70} . The data shown are for [A59C, R596C] σ^{70} . Insets in (A), (B), and (C) show the first 500 μ s of the decay curves. Solid lines show nonlinear regression of the data to the triple-exponential decay equation, as described in the text. (D) Decays of sensitized emission of acceptor for the same samples for which donor decays are shown in (A), (B), and (C): (open circles) free donor-acceptor σ^{70} ; (open triangles) core-bound donor-acceptor σ^{70} ; (closed triangles) dissociated donor-acceptor σ^{70} .

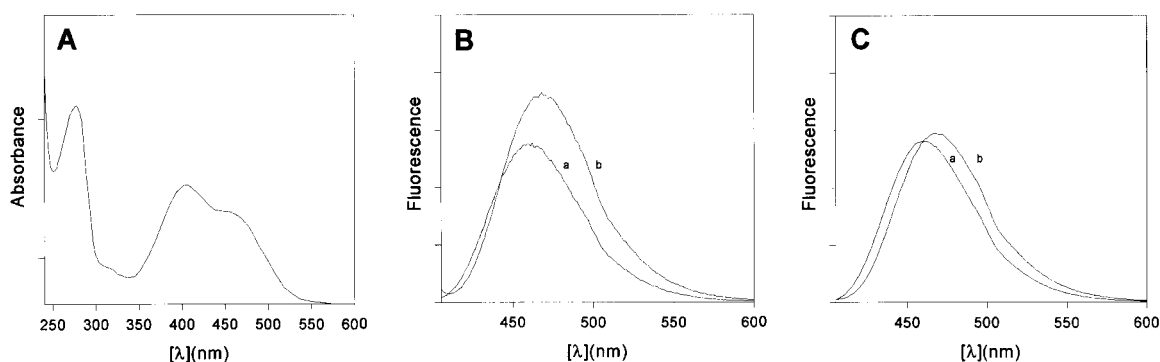


Figure 4. Fluorescence Energy Transfer in σ^{70} Labeled with CPM (Donor) and DABMI (Acceptor)

The data shown are for [T442C, R596C] σ^{70} . (A) Absorption spectrum of purified CPM and DABMI-labeled σ^{70} . (B) Fluorescence emission spectra of CPM and DABMI labeled (donor-acceptor-labeled) free σ^{70} (curve a) and σ^{70} bound to the core RNAP (curve b). (C) Fluorescence emission spectra of CPM-only (donor-only) labeled free σ^{70} (curve a) and σ^{70} bound to the core RNAP (curve b).

emission upon binding to the core RNAP (Figure 4B), indicating that a decrease of energy transfer between these probes occurred upon core binding since with donor-only σ^{70} only a small change of donor emission was observed (Figure 4C).

Specificity of Core-Induced Changes in Luminescence Properties of Labeled σ^{70}

The procedure for σ^{70} preparation involves a denaturation-renaturation step (Gribskov and Burgess, 1983; Callaci and Heyduk, 1998). Therefore, it is important to establish that labeled σ^{70} mutants obtained by such procedure are correctly folded and functional. Several observations suggest that labeled σ^{70} mutants were properly folded and formed a functional specific complex with the core polymerase.

Double-Cysteine Mutants of σ^{70} Were Active

Sites for introducing cysteine residues in double-cysteine mutants of σ^{70} were selected based on our previous experiments with single-cysteine mutants of σ^{70} (Callaci et al., 1998) such that cysteine incorporation should have a minimal effect on transcriptional activity of σ^{70} . Consistent with this selection strategy, the activity of double-cysteine mutants of σ^{70} used in this work was similar to the wt protein (75%–120% of wt activity; data not shown).

Donor- and Acceptor-Labeled σ^{70} Mutants Were Capable of Forming the Open Complex

After modification with donor and acceptor, the activity of σ^{70} mutants was significantly reduced (15%–50% of wt activity; data not shown). This reduction most likely was due to steric effects resulting from introducing fluorochromes into sites close to the residues directly involved in interactions with promoter DNA. Thus, this reduction in activity most likely occurs at the level of holoenzyme-promoter DNA binding, downstream from the events studied in this report (σ^{70} -core interactions). However, donor and acceptor-labeled proteins were a heterogeneous mixture of different species (Figure 1B). A possibility thus existed that in this mixture the species providing LRET signal (1 and 2 in Figure 1B) could be completely nonfunctional and inactive, and the reduced activity observed could be 100% due to the remaining

possible species. We have thus performed an experiment in which donor-acceptor-labeled σ^{70} mutants reconstituted to the holoenzyme were mixed with 114 bp unlabeled promoter fragment under conditions allowing open complex formation. The complexes formed were challenged with heparin, and stable open complexes were resolved using native polyacrylamide electrophoresis (Straney and Crothers, 1985). We determined that open complex bands in polyacrylamide gel exhibited fluorescence of Cy5, luminescence of Eu^{3+} , and sensitized fluorescence of Cy5 (data not shown). Thus, this experiment directly showed that donor-acceptor-labeled σ^{70} mutants were capable of open complex formation. Since formation of the open complex involves cooperation of many domains of σ^{70} , this result strongly argues that labeled σ^{70} mutants were properly folded functional proteins.

Donor-Acceptor-Labeled σ^{70} Bound the Core with a High Affinity

Figures 5A–5C show sizing column profiles of labeled σ^{70} in the presence of increasing amounts of core RNAP. The formation of labeled σ^{70} -core complex was apparent as shown by the appearance of a fluorescent peak co-eluting with the peak of core RNAP. The complexes between labeled σ^{70} and the core polymerase were able to survive repeated chromatography on the sizing column at low nanomolar concentrations indicating high affinity of the labeled σ^{70} for binding the core. Figure 5D shows a plot of the fraction of σ^{70} in a complex with core RNAP (as determined from sizing column experiments) as a function of molar ratio of core to σ^{70} in a sample loaded on a sizing column. The fraction of σ^{70} bound to the core increased until \sim 1:1 input ratio of core/ σ^{70} . The maximum amount of σ^{70} bound was 70%–90% for different preparations of labeled σ^{70} mutants. The change of the acceptor signal was found to correlate well with the amount of σ^{70} bound to core enzyme (Figure 5D). Thus, changes in luminescence of labeled σ^{70} in the presence of core were due to a formation of a specific 1:1 complex between σ^{70} and core RNAP.

Labeled σ^{70} Mutants and the WT σ^{70} Competed for the Same Binding Site in the Core Polymerase

Superdex 200-purified holoenzyme containing labeled σ^{70} was incubated with a 10-fold excess of unlabeled

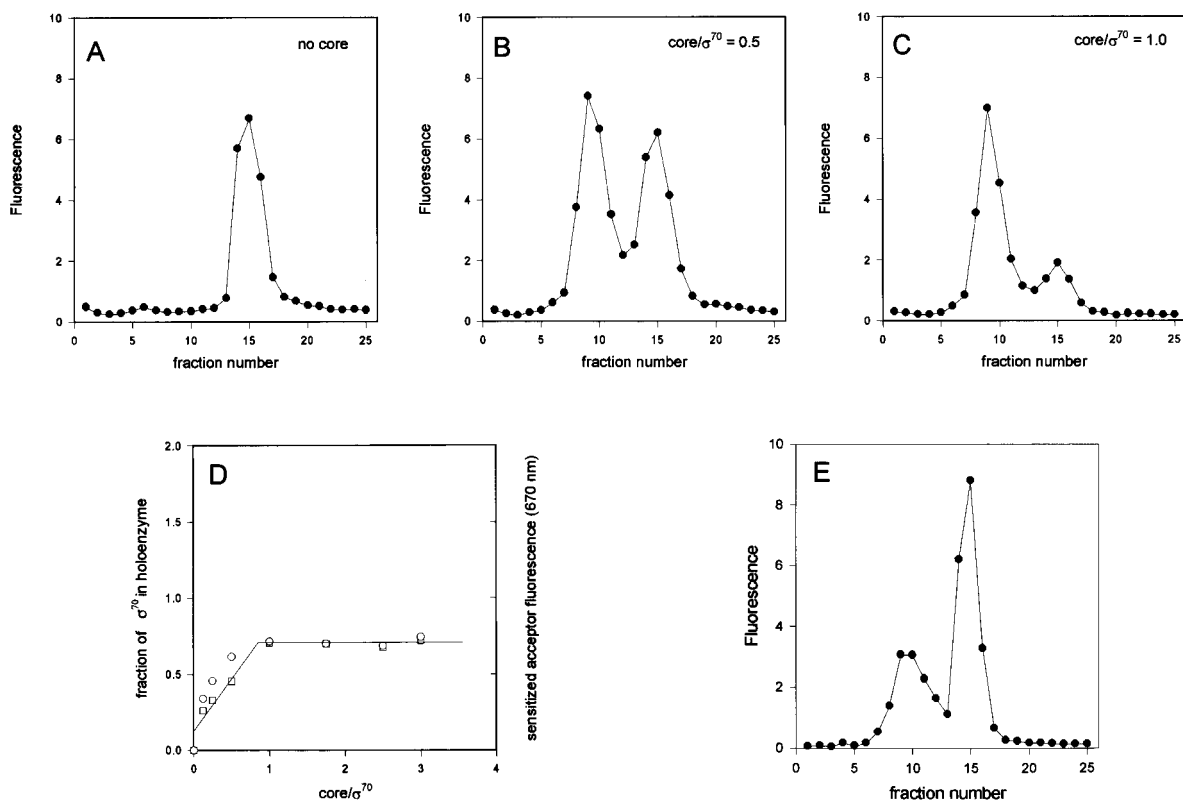


Figure 5. Correlation between Binding of Donor-Acceptor-Labeled σ^{70} to the Core RNAP and the Changes of Sensitized Emission of Acceptor The data shown are for [A59C, R596C] σ^{70} . (A) Superdex 200 elution profile of free donor-acceptor σ^{70} ; (B) Superdex 200 elution profile of donor-acceptor σ^{70} mixed with core at 0.5:1.0 molar ratio; (C) Superdex 200 elution profile of donor-acceptor σ^{70} mixed with core RNAP at 1:1 molar ratio. The elution of labeled σ^{70} was followed by fluorescence of Cy5 (excitation at 647 nm, emission at 670 nm). (D) A plot of fraction of σ^{70} bound to the core RNAP and sensitized acceptor fluorescence as a function of the molar ratio of core to σ^{70} . The fraction of σ^{70} bound to core RNAP was determined by running mixtures σ^{70} and the core RNAP on Superdex 200 and calculating a total fluorescence in fractions containing σ^{70} and the holoenzyme, respectively. The sensitized emission of acceptor was measured at 670 nm with pulsed excitation of the donor at 337 nm (N_2 laser). Sensitized emission was integrated for 1250 μ s with a delay of 250 μ s after the excitation pulse. (E) Release of labeled σ^{70} from the holoenzyme by competition with the wt σ^{70} . Superdex 200 profile of a holoenzyme sample incubated with a 10-fold excess of unlabeled σ^{70} is shown (details of the experiment are described in Experimental Procedures).

σ^{70} overnight, and the mixture was loaded on a Superdex 200 column. The majority of labeled σ^{70} was displaced from the holoenzyme as shown by the appearance of free labeled σ^{70} peak in a Superdex 200 column profile (Figure 5E). Peak fraction containing free σ^{70} (fraction #15, Figure 5E) was collected and was used for luminescence lifetime determination. The dissociated σ^{70} exhibited identical decay curve as observed with the free σ^{70} (Figure 3D). The experiment illustrated by Figure 5E showed a direct competition between wt and labeled σ^{70} for binding to the core. The experiment illustrated by Figure 3D indicated that labeled σ^{70} mutants were properly folded since the dissociated σ^{70} should not contain any improperly folded protein, as it was derived from only these σ^{70} molecules that exhibited the ability to bind to the core RNAP. Identical luminescence decays for free σ^{70} and dissociated σ^{70} were also obtained using a different method of dissociating labeled σ^{70} (chromatography of the holoenzyme containing labeled σ^{70} on a minicolumn with BioRex-70 attached to a minicolumn with DEAE-cellulose (Lowe et al., 1979; data not shown).

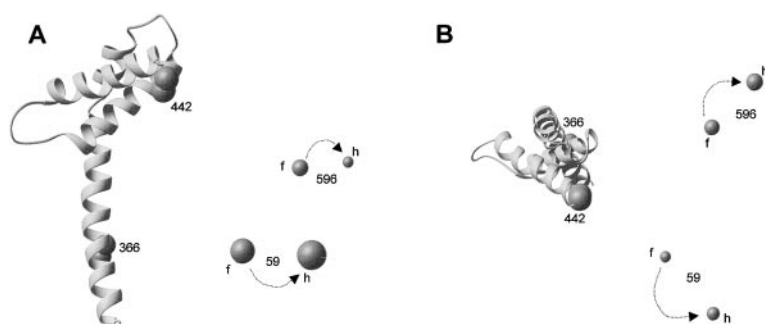
Labeled σ^{70} Proteins Exhibited the Same Pattern of Limited Digestion with Trypsin as Observed for the WT Protein

Susceptibility to limited proteolysis by trypsin is a sensitive test for overall folding of σ^{70} protein (Lowe et al., 1979; Callaci and Heyduk, 1998). With all labeled σ^{70} mutants, limited proteolysis with trypsin produced a characteristic protease-resistant 40 kDa fragment (data not shown) observed in the case of the wt protein (Lowe et al., 1979).

In summary, although none of the above control experiments by themselves conclusively prove that labeled σ^{70} mutants were properly folded and capable of specific and functional interaction with the core, taken together, these results strongly indicated that this was the case.

Discussion

We have measured all distances between four sites in free σ^{70} protein and in σ^{70} protein in complex with the



of residue 59 and residue 596 movement induced by the core. (A) and (B) show two views of the model differing by a rotation of $\sim 90^\circ$ around the x axis. The models were rendered using RIBBONS (Carson, 1991). The coordinates of the crystal structure of σ^{70} (Malhotra et al., 1996) were obtained from Brookhaven Protein Data Bank (accession code 1sig).

Figure 6. Three-Dimensional Models of σ^{70} Domain Architecture in Free σ^{70} and Core-Bound σ^{70}

The models were built as described in Experimental Procedures. A fragment of σ^{70} crystal structure (residues 355–446) is shown in ribbons representation whereas the positions of σ^{70} domains deduced from LRET measurements are shown as spheres. Positions of domains in free σ^{70} are indicated by a letter f whereas positions in the holoenzyme are indicated by a letter h. The rotation of LRET models around the 366–442 axis is arbitrary and was chosen for convenient visualization

core RNAP. The sites selected for these distance measurements are located in conserved domains of σ^{70} involved in recognition of -10 and -35 DNA sequences (residues 442 and 596, respectively), in a conserved domain of σ^{70} involved in autoinhibition of promoter DNA binding activity (residue 59), and in a nonconserved region of the protein in the vicinity of a putative core binding region σ^{70} (residue 366). The picture emerging from our distance measurements is that a major σ^{70} protein domain rearrangement takes place in response to binding of the core RNAP as indicated by large changes (increases) of interdomain distances observed upon σ^{70} -core RNAP complex formation.

In order to better understand the nature of the core-induced changes in σ^{70} , the three-dimensional models of domain architecture were built for free σ^{70} and for core-bound σ^{70} . Both in the case of free protein and the core-bound protein, self-consistent models (i.e., models in which all the distances between σ^{70} domains were identical to those measured by LRET) could be built. This provides some additional assurance that the distances measured by LRET are correct since only a limited combination of distances would allow building such self-consistent models. The built models were then superimposed on the σ^{70} fragment for which the three-dimensional structure is available (Malhotra et al., 1996) (Figure 6). The superimposition of the model with the crystal structure was possible because our distance measurements included two sites (residues 366 and 442) that were also present in the crystallized fragment of σ^{70} . Distances between these two sites measured by LRET both in free σ^{70} as well as in the holoenzyme were very similar to each other (35 Å and 39 Å) and also to a distance between these two sites in the crystal structure (~ 35 Å). Thus, in building the model we assumed that these sites are not affected by binding of the core enzyme. The spheres representing positions 366 and 442 in a model built based on LRET data were aligned with positions 366 and 442 in the structure of crystallized protein fragment, and the rest of the LRET model was rotated along the residue 366–residue 442 axis to obtain a configuration of the other domains such that no steric clash with the remainder of σ^{70} structure occurred. Finally, the relative positions of models for free σ^{70} and core-bound σ^{70} were set by rotating the models with

respect to each other along the residue 366–residue 442 axis until minimal differences in positions of residues 59 and 596 between free σ^{70} and core-bound σ^{70} were achieved. Thus, the final product of this model building shown in Figure 6 represents the simplest set of molecular motions sufficient to produce core-induced rearrangement of σ^{70} domains consistent with LRET data. These molecular motions include a movement of only two domains: translation of region 1 (residue 59) by ~ 20 Å and region 4.2 (residue 596) by ~ 15 Å in directions illustrated by arrows in Figure 6. Thus, although five out of six measured distances were found to increase upon core RNAP binding (Tables 1 and 2), only movement of two domains was necessary to model the observed distance changes. Domain movements in σ^{70} are large, but domain motions of this magnitude and larger (up to ~ 60 Å) were observed in other systems (Gernstein and Krebs, 1998).

The changes induced in σ^{70} by the core polymerase were modeled in Figure 6 as a rigid body movement (translation) of the domains. This, however, is not the only possible mechanism by which distance changes observed by LRET could be obtained. Alternative interpretation of observed distance changes could involve more complex movements such as relative rotation of the domains or a combination of rotation and translation. Another interesting possibility could be that the core induced changes in the flexibility of σ^{70} . Since the lifetime of the donor used for LRET measurements was in a microsecond range, the distances determined most likely corresponded to a distance of the closest approach between the donor and the acceptor. Thus, an apparent increase of several interdomain distances in σ^{70} induced by core could be a result of a decrease in flexibility of σ^{70} in the holoenzyme. Although the observation of similar LRET effects induced by core polymerase using probes with nanosecond lifetimes argues against this interpretation (Figure 4), it does not rule out completely the possibility that flexibility changes play some role in observed interdomain distance changes. There is now a well-documented example of the importance of domain flexibility for the function of RNAP—the C-terminal domain of α subunit (Ebright and Busby, 1995). Interestingly, the anti-sigma factor FlgM, which binds to and inhibits σ^{28} and which was suggested to

play the role analogous to the region 1 of σ^{70} , was shown to be disordered in solution and partially ordered in complex with σ^{28} (Daughdrill et al., 1998). We are currently attempting to determine the flexibility of σ^{70} domains in free protein and in the holoenzyme. Whatever the precise nature of core-induced domain movement might be, the two important conclusions are that the core induces a movement of region 1 away from DNA-binding domains and that the core induces repositioning of DNA-binding domains.

The major motivation for undertaking the studies described in this report was to test the hypothesis that binding of the core RNAP induces a movement of region 1 to unmask DNA-binding domains of σ^{70} . This hypothesis was derived from the model proposed by Dombroski et al. (1993b) to explain why free σ^{70} could not bind promoter DNA. Our results suggest a major movement of region 1 (residue 59) induced by core binding. We have shown previously that core RNAP induces an increase in solvent accessibility of residues in region 4.2 (Callaci et al., 1998). Both these results are consistent with the unmasking nature of core-induced conformational transition in σ^{70} and with the important role of region 1 in this transition. Our result suggests also an additional mechanism for regulation of promoter binding activity of σ^{70} by core RNAP. The distance between region 2.4 (residue 442) and region 4.2 (residue 596) was ~ 35 Å in free σ^{70} . Regions 2.4 and 4.2 are thought to interact with two regions of promoter DNA separated by a ~ 17 bp spacer. The distance between regions 2.4 and 4.2 in free σ^{70} is much too small to allow a simultaneous interaction of these two regions with corresponding DNA sites. The distance between region 2.4 and 4.2 is increased to ~ 50 Å in the holoenzyme, a distance much more compatible with ~ 17 bp separation between binding sites in DNA. Experimental evidence for the role of σ^{70} in sensing the spacing between the -10 and -35 region of promoter DNA was recently presented (Dombroski et al., 1996). Therefore, our results suggest that DNA binding activity of σ^{70} could also be regulated through a modulation of spacing between DNA-binding domains of the protein induced by binding of core RNAP. As already discussed, the distance change between DNA-binding domains could also occur as a result of a more complex movement (e.g., rotation of domains). Such interpretation would also lead to a conclusion that DNA binding activity of σ^{70} is regulated by the core through repositioning of DNA-binding domains, although the nature of this repositioning would be more complex than a simple "spacing sensing" described above.

Our data provided direct evidence for a large scale domain rearrangement in σ^{70} induced by core RNAP binding. Functionally important domain motions in proteins in response to ligand binding have been observed in many systems (Gernstein and Krebs, 1998). The experimental strategy presented in this report—a combination of site-directed mutagenesis and energy transfer measurements enhanced through the use of lanthanide chelate probes—could generally be used in other systems, especially in complicated multiprotein complexes as the RNAP holoenzyme studied in this report.

Experimental Procedures

Materials

7-diethylamino-3-(4'-maleimidylphenyl)-4-methylcoumarin (CPM) (Sipel, 1981), 4-dimethylaminophenylazophenyl-4'-maleimide (DABMI) (Chang et al., 1983) were from Molecular Probes, Inc. (Eugene, OR). Monosuccinimidyl ester of Cy5 (Mujumdar et al., 1993) was purchased from Amersham (Arlington Heights, IL). The succinimidyl ester of Cy5 was converted to maleimide as described previously (Callaci et al., 1998). (Eu^{3+}) DTPA-AMCA-maleimide, the luminescent donor used in LRET experiments, was prepared as described (Heyduk and Heyduk, 1998). *Escherichia coli* K12 cell paste was obtained from the University of Alabama Fermentation Facility. All other chemicals were of the highest purity commercially available.

Double-Cysteine Mutants of σ^{70}

The plasmid containing *rpoD* gene for the wt σ^{70} was a gift from Dr. Akira Ishihama (National Institute of Genetics, Mishima, Japan). The double-cysteine mutants of σ^{70} were constructed from single-cysteine mutants of σ^{70} described previously (Callaci et al., 1998). The mutants were obtained by exchanging appropriate unique restriction site fragments between corresponding single-cysteine σ^{70} mutant DNA. [A59C, S442C] σ^{70} , [A59C, S366C] σ^{70} mutants were made by replacing a SacII-Clal fragment of [A59C] σ^{70} mutant with SacII-Clal fragments of [S442C] σ^{70} and [S366C] σ^{70} mutants, respectively. [S366C, R596C] σ^{70} and [S442C, R596C] σ^{70} mutants were made by replacing a SacII-Clal fragment of [R596C] σ^{70} mutant with SacII-Clal fragments of [S442C] σ^{70} and [S366C] σ^{70} mutants, respectively. The [A59C, R596C] σ^{70} mutant was made by replacing Clal-Nsil fragment of [R596C] σ^{70} mutant with Clal-Nsil fragment of [A59C] σ^{70} mutant. The [S366C, S442C] σ^{70} mutant was made by replacing BstBI-NcoI fragment of [S366C] σ^{70} mutant with BstBI-NcoI fragment of [S442C] σ^{70} mutant. To replace the fragments, the appropriate plasmids were digested with restriction enzymes, the resulting fragments were purified by agarose gel electrophoresis, and the appropriate fragments were ligated by T4 DNA ligase. The identity of all mutants was confirmed using dideoxy DNA sequencing method (Sanger et al., 1977). The σ^{70} protein expression, purification, limited proteolysis with trypsin, and transcriptional activity were performed as described previously (Callaci and Heyduk, 1998).

Core RNAP was purified from *E. coli* K12 cells using the method of Burgess and Jendrisak (1975) utilizing chromatography on DNA-cellulose, Sephacryl 300 HR, and Bio-Rex 70 anion exchange column (Bio-Rad Laboratories, Richmond, CA).

Labeling of σ^{70} Mutants with Donor and Acceptor

Fluorescence Probes

Samples of each double-cysteine mutant of σ^{70} (0.5–1.0 mg) were precipitated with 60% ammonium sulfate by the addition of the appropriate volume of saturated ammonium sulfate solution. Protein pellet was collected by centrifugation and dissolved in 75 μl of 50 mM Tris (pH 8.0), 1 mM EDTA, 5% glycerol containing 6 M GdHCl. DTT was added to a final concentration of 0.5 mM, and mixtures were incubated for 1 hr at room temperature. DTT was removed by a microspin G-50 column (Pharmacia) equilibrated with the above buffer. DTPA-AMCA-maleimide was added such that the molar ratio of DTPA-AMCA-maleimide to σ^{70} cysteines was ~ 0.4 . The reaction was allowed to proceed for 1 hr at room temperature. Cy5 maleimide was then added in excess (1 mM), and the reaction was allowed to continue for another 2 hr. When samples of σ^{70} labeled with donor-only were prepared, a modification with nonfluorescent n-ethylmaleimide was performed in place of the Cy5 maleimide modification step. The reaction was stopped by addition of 1 mM DTT. The excess of unreacted fluorochromes was removed by a microspin G-50 column equilibrated with 50 mM Tris (pH 8.0), 1 mM EDTA, 5% glycerol containing 6 M GdHCl. The eluate from G-50 column was diluted to ~ 0.75 ml with the above buffer, dialyzed first against 100 ml of the same buffer for a few hours, and next against 50 mM Tris (pH 8.0), 5% glycerol buffer overnight with three changes of 100 ml of the buffer. Refolded proteins were incubated for 15 min with slight excess of Eu^{3+} and were purified from aggregates on a Superdex 200 FPLC sizing column (Pharmacia). Labeling of σ^{70} with

CPM and DABMI was performed as described above for DTPA-AMCA-maleimide and Cy5 maleimide modification.

Dissociation of Fluorochrome-Labeled σ^{70} from the Holoenzyme by Competition with Native σ^{70}

Holoenzyme (0.25 μ M) containing fluorochrome-labeled σ^{70} purified on Superdex 200 FPLC sizing column was incubated overnight at 4°C with 2.5 μ M native unlabeled σ^{70} in 400 μ l of 50 mM Tris/HCl (pH 8.0), 0.25 M NaCl, 5% glycerol. The mixture (200 μ l) was loaded onto Superdex 200 FPLC sizing column, and the fractions containing free fluorochrome-labeled σ^{70} were collected and were used for fluorescence experiments.

Dissociation of Fluorochrome-Labeled σ^{70} from the Holoenzyme Using Bio-Rex 70/DEAE Cellulose Chromatography

The dissociation of holoenzyme by Bio-Rex 70/DEAE cellulose chromatography was performed based on the method described by Lowe et al. (1979). The holoenzyme containing fluorochrome-labeled σ^{70} was formed by mixing 2.5 μ M core RNAP with 3.7 μ M labeled σ^{70} in 200 μ l of 50 mM Tris/HCl (pH 8.0), 250 mM NaCl. After incubation for 15 min at room temperature, the mixture was loaded on a Superdex 200 FPLC sizing column, and the fractions (~1.5 ml) containing the holoenzyme were diluted to 0.1 M NaCl with 50 mM Tris/HCl (pH 8.0), 5% glycerol. The holoenzyme solution (3.75 ml) was loaded on a 1 ml Bio-Rex 70 column attached to a 0.1 ml column with DEAE cellulose. Both columns were equilibrated with 50 mM Tris/HCl (pH 8.0), 0.1 M NaCl, 5% glycerol. The columns were washed with 5 ml of the starting buffer. The DEAE cellulose column was disconnected, and the dissociated fluorochrome-labeled σ^{70} captured by the DEAE column was eluted with 300 μ l of the buffer containing 0.5 M NaCl. The fractions eluted from DEAE cellulose column were loaded onto a Superdex 200 FPLC sizing column. Fractions containing free fluorochrome-labeled σ^{70} were collected and were used for fluorescence experiments.

Steady-State Fluorescence Measurements

Steady-state fluorescence emission spectra were recorded on a SLM 500C (SLM Instruments, Urbana, IL) or on an AmincoBowman Series 2 spectrofluorometer (Spectronic Instruments, Rochester, NY). Spectra were corrected for background using buffer-only samples. Fluorescence polarization measurements were performed on SLM 500C spectrofluorometer equipped with a polarization accessory.

Time-Resolved Luminescence Measurements

Luminescence lifetime measurements were performed on a laboratory-built two-channel spectrofluorometer with a pulsed nitrogen laser (LN300, Laser Photonics, Orlando) as an excitation source (Heyduk and Heyduk, 1997). The measurements were performed in a 120 μ l cuvette in 50 mM Tris/HCl (pH 8.0), 250 mM NaCl, 5% glycerol buffer at 25°C. Concentration of labeled proteins was 10–75 nM. Donor emission was observed at 617 nm using 620 nm, 10 nm bandwidth interference filter (Oriel, Stratford, CT) whereas acceptor emission was observed at 670 nm using 670 nm, 10 nm bandwidth interference filter (Oriel, Stratford, CT). The decays for donor-only samples were monoexponential and were analyzed according to $I(t) = \alpha \exp(-t/\tau)$ (Equation 1), where α is the amplitude of the decay and τ is the luminescence lifetime. Decays of donors in the presence of acceptor and decays of sensitized acceptor emission were three exponential. The interpretation of the observed decay times is presented in the Results section. Donor and sensitized acceptor decay curves were fitted simultaneously using global nonlinear regression with SCIENTIST (Micromath Scientific Software, Salt Lake City, UT) to the following set of equations (Equation 2):

$$I_d(t) = \sum \alpha_{i,d} \exp(-t/\tau_i)$$

$$I_a(t) = \sum \alpha_{i,a} \exp(-t/\tau_i)$$

where $I_d(t)$ and $I_a(t)$ are luminescence intensity of donor and sensitized acceptor, respectively, $\alpha_{i,d}$ and $\alpha_{i,a}$ are amplitudes of the i^{th} component in donor and sensitized acceptor decay, respectively,

and τ_i is the lifetime of the i^{th} component. Such global fitting is possible due to unique characteristics of europium chelate-Cy5 donor-acceptor pair (long microsecond lifetime of the donor and nanosecond lifetime of the acceptor). The decay of sensitized acceptor in a microsecond time scale occurs with the lifetime(s) of the donor engaged in energy transfer with the acceptor (Selvin, 1996; Heyduk and Heyduk, 1997). Thus, the decays of the donor and sensitized acceptor are described by the same lifetimes but different amplitudes (Equation 2).

LRET Calculations

The energy transfer (E) was calculated from measurements of luminescence lifetime of a donor in the absence (τ_d) and in the presence of acceptor (τ_{da}): $E = 1 - \tau_{da}/\tau_d$. The distances between donor and acceptor were calculated according to Förster (1948): $R^6 = R_0^6(1 - E)/E$, where R is a distance between a donor and an acceptor, and R_0 is a distance at which the energy transfer is 0.5. The R_0 for (Eu³⁺)DTPA-AMCA and Cy5 donor-acceptor pair (55 Å) was calculated as described previously (Heyduk and Heyduk, 1997). In calculating R_0 , a completely randomized orientation of donor and acceptor fluorochromes was assumed (Selvin and Hearst, 1994; Selvin et al., 1994; Selvin, 1996; Heyduk and Heyduk, 1997).

Model Building

Models of the three-dimensional architecture of σ^{70} domains were built using the distance constraint routine of ChemSite (Pyramid Learning, Stanford, CA). The models were superimposed on the crystal structure of σ^{70} fragment (Malhotra et al., 1996) using MIDAS (Ferrin et al., 1988) (Computer Graphics Laboratory, University of California, San Francisco, supported by NIH P41 RR-01081) by manually aligning residues 442 and 366 of the crystal structure with spheres representing positions 442 and 366 of the models built based on LRET data. The final rendering was done using RIBBONS (Carson, 1991).

Acknowledgments

This work was supported by a grant from National Institutes of Health (GM50514).

Received September 28, 1998; revised December 15, 1998.

References

- Burgess, R.R., and Jendrisak, J.J. (1975). A procedure for the rapid, large-scale purification of *Escherichia coli* DNA-dependent RNA polymerase involving polymin P precipitation and DNA-cellulose chromatography. *Biochemistry* 14, 4634–4638.
- Burgess, R.R., and Travers, A.A. (1970). *Escherichia coli* RNA polymerase: purification, subunit structure, and factor requirements. *Fed. Proc.* 29, 1164–1169.
- Burgess, R.R., Travers, A.A., Dunn, J.J., and Bautz, E.K. (1969). Factor stimulating transcription by RNA polymerase. *Nature* 221, 43–46.
- Callaci, S., and Heyduk, T. (1998). Conformation and DNA binding properties of a single-stranded DNA binding region of sigma 70 subunit from *Escherichia coli* RNA polymerase are modulated by an interaction with the core enzyme. *Biochemistry* 37, 3312–3320.
- Callaci, S., Heyduk, E., and Heyduk, T. (1998). Conformational changes of *E. coli* RNA polymerase σ^{70} factor induced by binding to the core enzyme. *J. Biol. Chem.* 273, 32995–33001.
- Carson, M. (1991). Ribbons 2.0. *J. Appl. Crystallogr.* 24, 958–961.
- Chang, J.Y., Knecht, R., and Braun, D.G. (1983). A new method for the selective isolation of cysteine-containing peptides. Specific labelling of the thiol group with a hydrophobic chromophore. *Biochem. J.* 211, 163–171.
- Daughdrill, G.W., Hanely, L.J., and Dahlquist, F.W. (1998). The C-terminal half of the anti-sigma factor FlgM contains a dynamic equilibrium solution structure favoring helical conformations. *Biochemistry* 37, 1076–1082.

- Dombroski, A.J., Walter, W.A., Record, M.T., Jr, Siegele, D.A., and Gross, C.A. (1992). Polypeptides containing highly conserved regions of transcription initiation factor sigma 70 exhibit specificity of binding to promoter DNA. *Cell* **70**, 501-512.
- Dombroski, A.J., Walter, W.A., and Gross, C.A. (1993a). Amino-terminal amino acids modulate sigma-factor DNA-binding activity. *Genes Dev.* **7**, 2446-2455.
- Dombroski, A.J., Walter, W.A., and Gross, C.A. (1993b). The role of the sigma subunit in promoter recognition by RNA polymerase. *Cell. Mol. Biol. Res.* **39**, 311-317.
- Dombroski, A.J., Johnson, B.D., Lonetto, M., and Gross, C.A. (1996). The sigma subunit of *Escherichia coli* RNA polymerase senses promoter spacing. *Proc. Natl. Acad. Sci. USA* **93**, 8858-8862.
- Ebright, R.H., and Busby, S. (1995). The *Escherichia coli* RNA polymerase alpha subunit: structure and function. *Curr. Opin. Genet. Dev.* **5**, 197-203.
- Ferrin, T.E., Huang, C.C., Jarvis, L.E., and Langridge, R. (1988). The MIDAS display system. *J. Mol. Graph.* **6**, 13-27.
- Forster, T. (1948). Zwischenmolekulare Energiewanderung und Fluoreszenz. *Ann. Phys.* **2**, 55-75.
- Gernstein, M., and Krebs, W. (1998). A database of macromolecular motions. *Nucleic Acids Res.* **26**, 4280-4290.
- Gribskov, M., and Burgess, R.R. (1983). Overexpression and purification of the sigma subunit of *Escherichia coli* RNA polymerase. *Gene* **26**, 109-118.
- Heyduk, E., and Heyduk, T. (1997). Thiol-reactive, luminescent europium chelates: luminescence probes for resonance energy transfer distance measurements in biomolecules. *Anal. Biochem.* **248**, 216-227.
- Heyduk, E., and Heyduk, T. (1999). Architecture of a complex between σ^{70} subunit of *E. coli* RNA polymerase and the nontemplate strand oligonucleotide: luminescence resonance energy transfer study. *J. Biol. Chem.* **274**, 3315-3322.
- Hinkle, D.C., and Chamberlin, M.J. (1972). Studies of the binding of *Escherichia coli* RNA polymerase to DNA. I. The role of sigma subunit in site selection. *J. Mol. Biol.* **70**, 157-185.
- Lonetto, M., Gribskov, M., and Gross, C.A. (1992). The sigma 70 family: sequence conservation and evolutionary relationships. *J. Bacteriol.* **174**, 3843-3849.
- Lowe, P.A., Hager, D.A., and Burgess, R.R. (1979). Purification and properties of the sigma subunit of *Escherichia coli* DNA-dependent RNA polymerase. *Biochemistry* **18**, 1344-1352.
- Malhotra, A., Severinova, E., and Darst, S.A. (1996). Crystal structure of a sigma 70 subunit fragment from *E. coli* RNA polymerase. *Cell* **87**, 127-136.
- Mujumdar, R.B., Ernst, L.A., Mujumdar, S.R., Lewis, C.J., and Waggoner, A.S. (1993). Cyanine dye labeling reagents: sulfoindocyanine succinimidyl esters. *Bioconj. Chem.* **4**, 105-111.
- Record, M.T., Jr, Reznikoff, W.S., Craig, M.L., McQuade, K.L., and Schlax, P.J. (1996). *Escherichia coli* RNA polymerase ($E\sigma^{70}$), promoters, and the kinetics of the steps of transcription initiation. In *Escherichia coli and Salmonella: Cellular and Molecular Biology*, 2nd ed., F.C. Neidhardt, R. Curtis III, J.L. Ingraham, E.C.C. Lin, K.R. Low, B. Magasanik, W.S. Reznikoff, M. Riley, M. Schaechter, and H.E. Umbarger, eds. (Washington, DC: ASM Press), 792-820.
- Sanger, F., Nicklen, S., and Coulson, A.R. (1977). DNA sequencing with chain-terminating inhibitors. *Proc. Natl. Acad. Sci. USA* **74**, 5463-5467.
- Selvin, P.R. (1995). Fluorescence resonance energy transfer. *Methods Enzymol.* **246**, 300-334.
- Selvin, P.R. (1996). Lanthanide-based resonance energy transfer. *IEEE J. Select Top. Quant. Electron.* **2**, 1077-1087.
- Selvin, P.R., and Hearst, J.E. (1994). Luminescence energy transfer using a terbium chelate: improvements on fluorescence energy transfer. *Proc. Natl. Acad. Sci. USA* **91**, 10024-10028.
- Selvin, P.R., Rana, T.M., and Hearst, J.E. (1994). Luminescence energy transfer. *J. Am. Chem. Soc.* **116**, 6029-6030.
- Sippel, T.O. (1981). New fluorochromes for thiols: maleimide and iodoacetamide derivatives of a 3-phenylcoumarin fluorophore. *J. Histochem. Cytochem.* **29**, 314-316.
- Straney, D.C., and Crothers, D.M. (1985). Intermediates in transcription initiation from the *E. coli lac uv5* promoter. *Cell* **43**, 449-459.
- Wellman, A., and Meares, C.F. (1991). Footprint of the sigma protein: a re-examination. *Biochem. Biophys. Res. Comm.* **177**, 140-144.
- Wu, F.Y., Yarbrough, L.R., and Wu, C.W. (1976). Conformational transition of *Escherichia coli* RNA polymerase induced by the interaction of sigma subunit with core enzyme. *Biochemistry* **15**, 3254-3258.